# Single-spin asymmetries in *e*-*p* scattering with intermediate state resonances

Peter Blunden (University of Manitoba)

SPIN 2023, September 2023

Collaborators: Jaseer Ahmed and Wally Melnitchouk

# Outline

- Single spin asymmetries (SSA): beam normal $B_n$ and target normal $A_n$ cases: absorptive **imaginary** part of two-photon exchange (TPE)
  - What can we learn from $B_n$ vs $A_n$
- Relationship to TPE calculations for elastic $e$-$p$ scattering cross sections and the ratio $G_E/G_M$ : dispersive **real** part of TPE
- Real and Imaginary parts connected by dispersion relations

# Dispersive method

Unitarity $\rightarrow$ $$\boxed{\mathrm{Im}\langle f|\mathcal{M}|i\rangle \sim \sum_n \int dW_n\, dQ_1^2\, dQ_2^2\ \langle f|\mathcal{M}^*|n\rangle\langle n|\mathcal{M}|i\rangle}$$

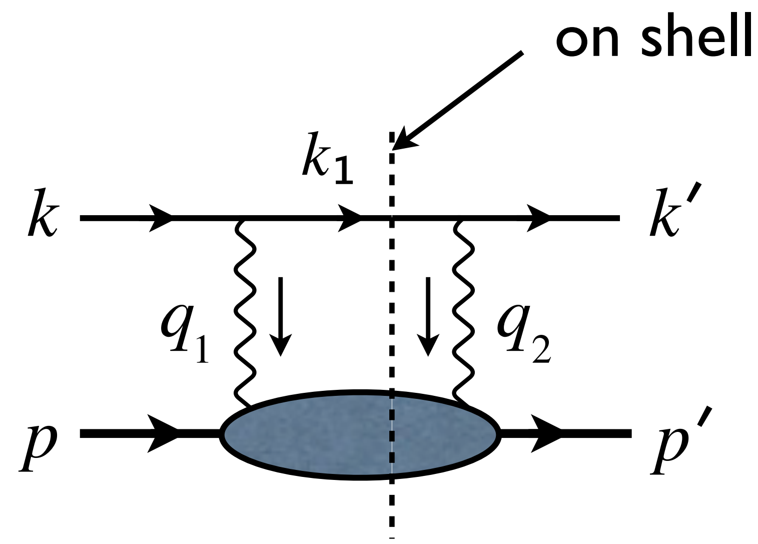


- Imaginary part determined by unitarity
- Uses only on-shell form factors (or helicity amplitudes), directly fit to data
- Real part determined from dispersion relations

- Resonance intermediate states:

$$\Delta(1232)3/2^+,\ N(1440)1/2^+,\ N(1520)3/2^-,\ N(1535)1/2^-,$$
$$\Delta(1620)1/2^-,\ N(1650)1/2^-,\ \Delta(1700)3/2^-,\ N(1710)1/2^+,\ N(1720)3/2^+$$

- CLAS exclusive meson electroproduction data for helicity amplitudes

$$A_{1/2},\ A_{3/2},\ S_{1/2}$$

- Include Breit-Wigner lineshape

# CLAS helicity amplitudes: Δ(1232), N(1440), N(1520)

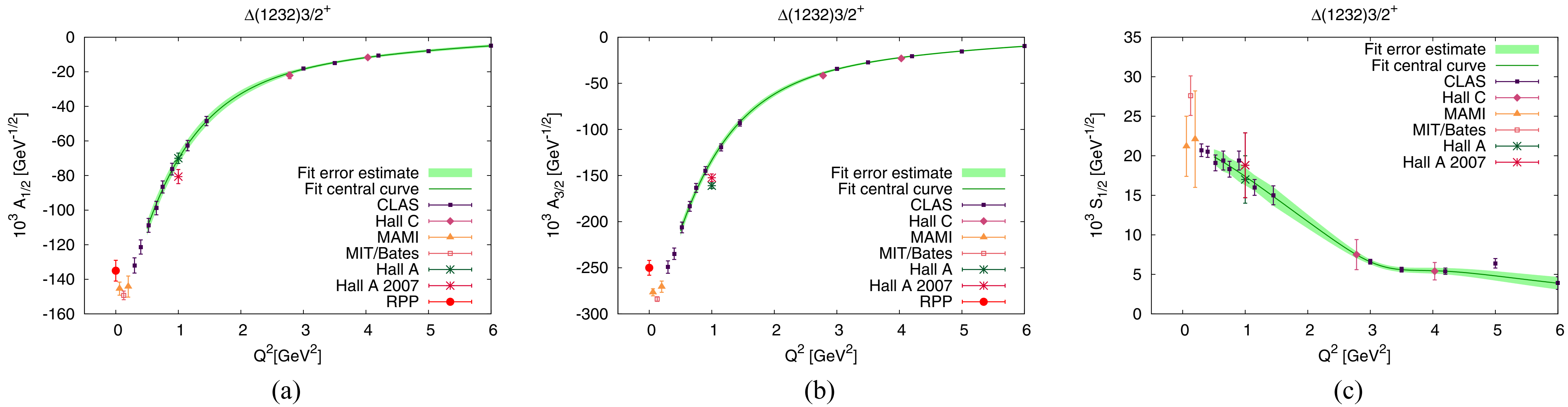


Hiller Blin *et al.*, PRC**100**, 035201 (2019)

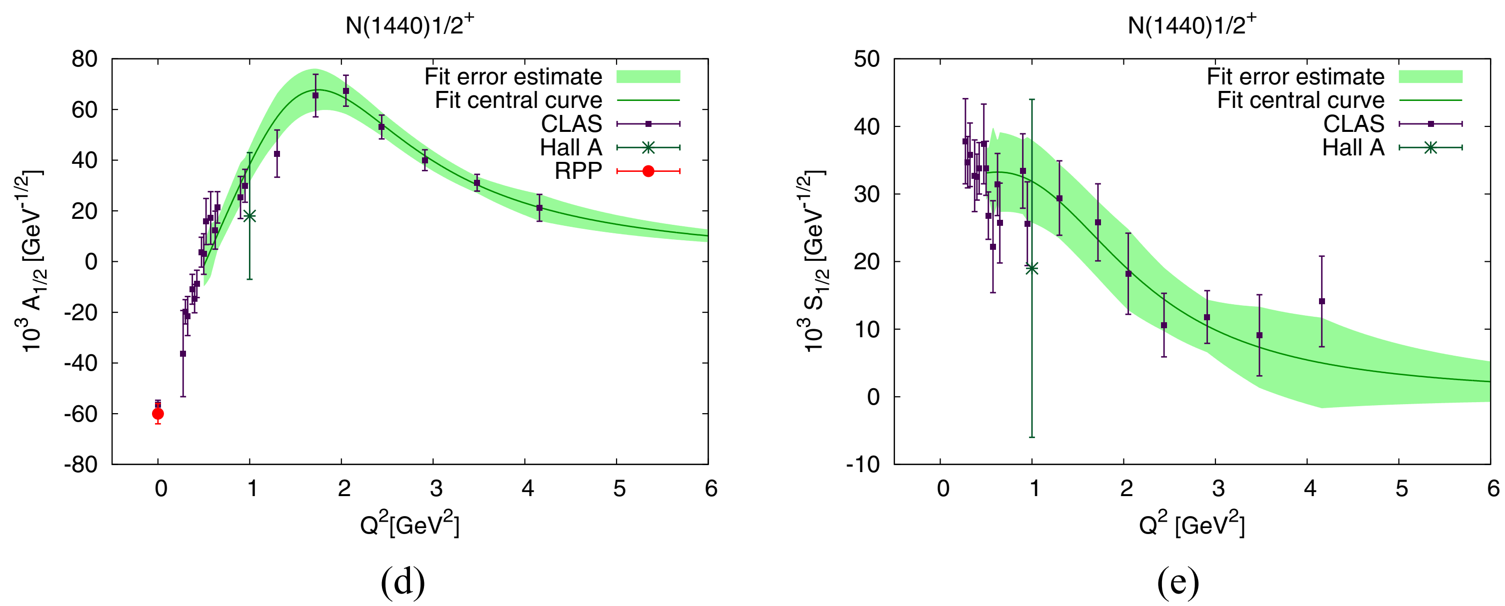


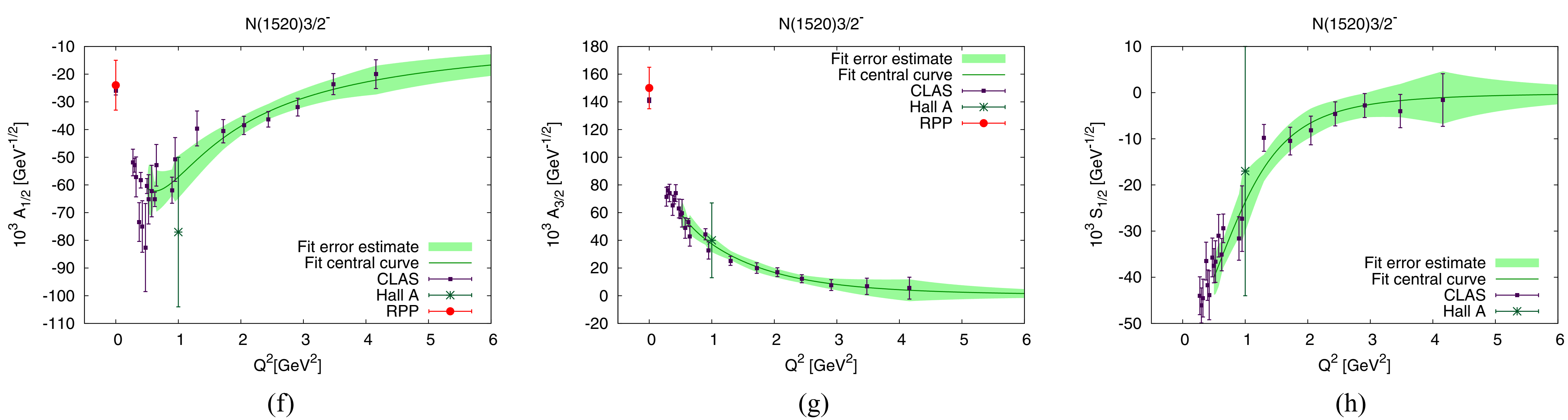

# CLAS unpolarized cross sections vs $W^2$

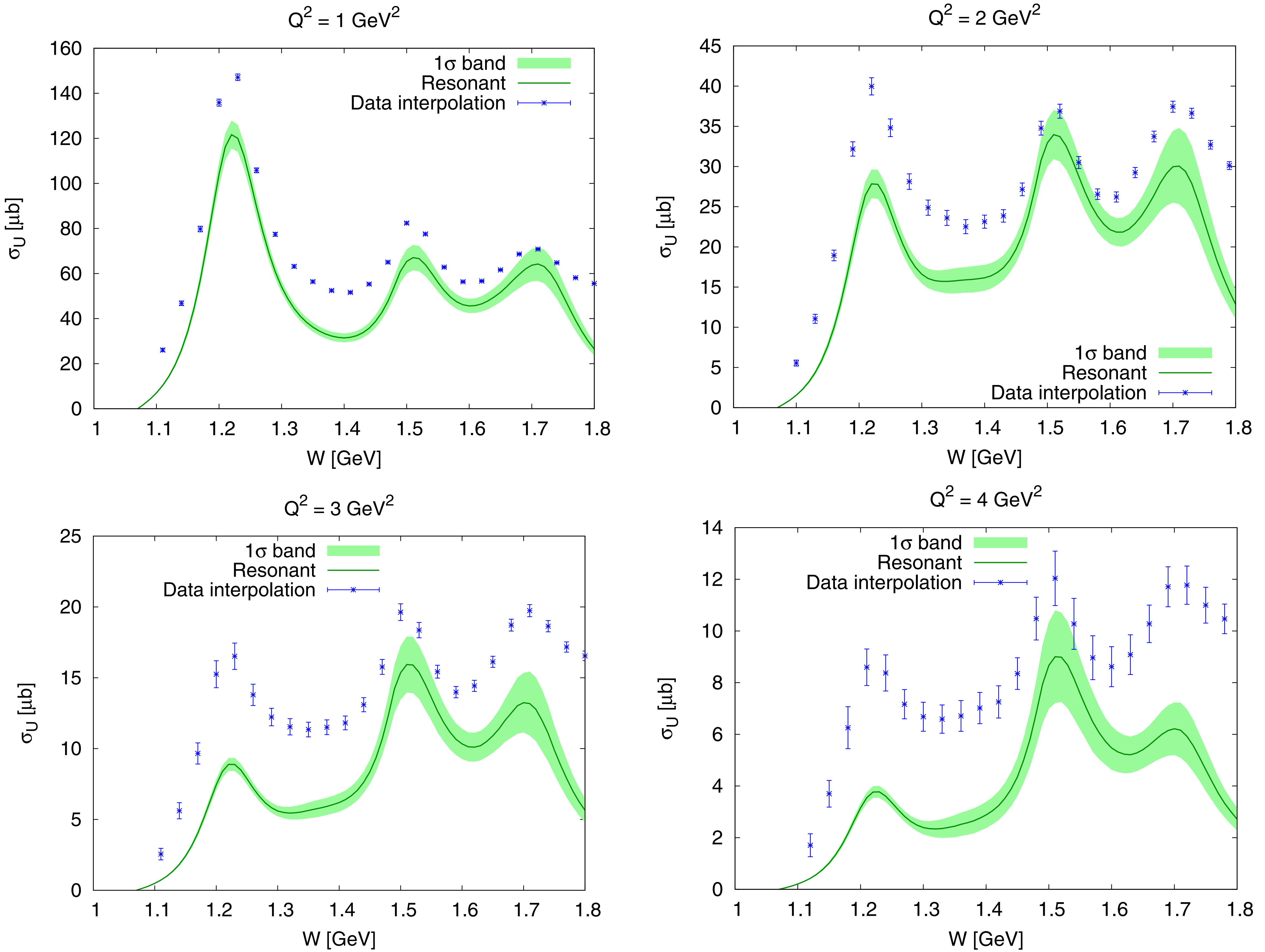


- Resonant vs. Total cross section at increasing $Q^2$

# TPE using dispersion relations

## Generalized form factors

$$\mathcal{M}_{\gamma\gamma} \to (\gamma_\mu)^{(e)} \otimes \left( F_1'(Q^2,\nu)\gamma^\mu + F_2'(Q^2,\nu)\frac{i\sigma^{\mu\nu}q_\nu}{2M} \right)^{(p)}$$
$$+ (\gamma_\mu\gamma_5)^{(e)} \otimes \left( G_a'(Q^2,\nu)\gamma^\mu\gamma_5 \right)^{(p)}$$

$$\delta_{\gamma\gamma} = 2\mathrm{Re}\, \frac{\varepsilon G_E(F_1' - \tau F_2') + \tau G_M(F_1' + F_2') + \nu(1-\varepsilon)G_M G_a'}{\varepsilon G_E^2 + \tau G_M^2}$$

## Dispersion relations

$$\mathrm{Re}\; F_1'(Q^2,\nu) = \frac{2}{\pi}\mathcal{P}\int_{-\tau}^{\infty} d\nu'\; \frac{\nu}{\nu'^2 - \nu^2}\,\mathrm{Im}\; F_1'(Q^2,\nu')\,,$$
$$\mathrm{Re}\; F_2'(Q^2,\nu) = \frac{2}{\pi}\mathcal{P}\int_{-\tau}^{\infty} d\nu'\; \frac{\nu}{\nu'^2 - \nu^2}\,\mathrm{Im}\; F_2'(Q^2,\nu')\,,$$
$$\mathrm{Re}\; G_a'(Q^2,\nu) = \frac{2}{\pi}\mathcal{P}\int_{-\tau}^{\infty} d\nu'\; \frac{\nu'}{\nu'^2 - \nu^2}\,\mathrm{Im}\; G_a'(Q^2,\nu')\,.$$

Integral extends into ``unphysical region'' down to zero energy ($\cos\theta < -1$)

# Direct measurements of Im part

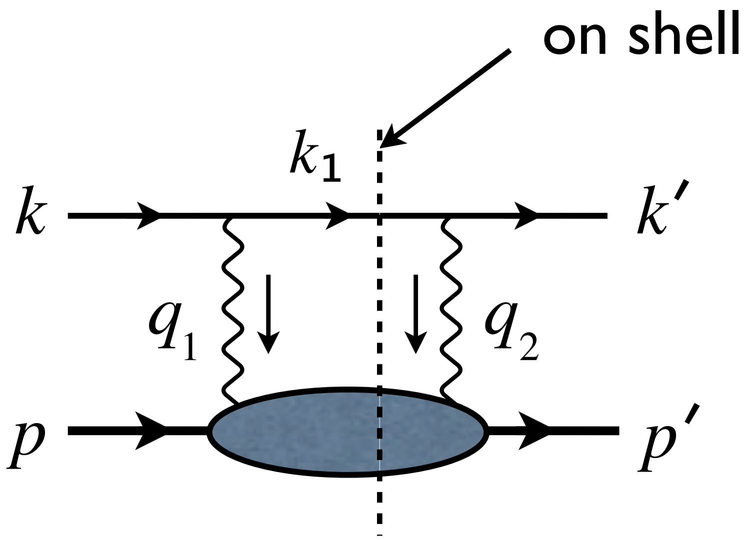


This is all in the physical region.

Target normal spin asymmetry: same FFs

$$A_n = \sqrt{2\epsilon(1+\epsilon)\tau}\ \frac{1}{\sigma_R} \mathrm{Im}\left\{ -G_M(F_1' - \tau F_2' + \nu F_3') \right.$$
$$\left. + G_E(F_1' + F_2' + \sqrt{\frac{2\epsilon}{1+\epsilon}} \nu F_3' \right\}$$

Beam normal spin asymmetry: additional dependence on spin-flip FFs

$$B_n = -\frac{m_e}{M} \sqrt{2\epsilon(1-\epsilon)(1+\tau)}\ \frac{1}{\sigma_R} \mathrm{Im}\left\{ \tau G_M F_3' + G_E F_4' + \nu F_1 F_5' \right\}$$

Probe different aspects of TPE!

# Ingredients of the calculation

$$\mathrm{SSA} = -\frac{\alpha\, Q^2}{\pi D(s,Q^2)} \int_{M^2}^{W^2_{\max}} dW^2\, \frac{|\vec{k}_1|}{4\sqrt{s}} \int_{-1}^{1} d\cos\theta_{k_1} \int_0^{2\pi} d\phi_{k_1}\, \frac{\mathrm{Im}\, L_{\rho\mu\nu} H^{\rho\mu\nu}}{Q_1^2\, Q_2^2}.$$

## Kinematic bounds on $Q_1^2$ and $Q_2^2$

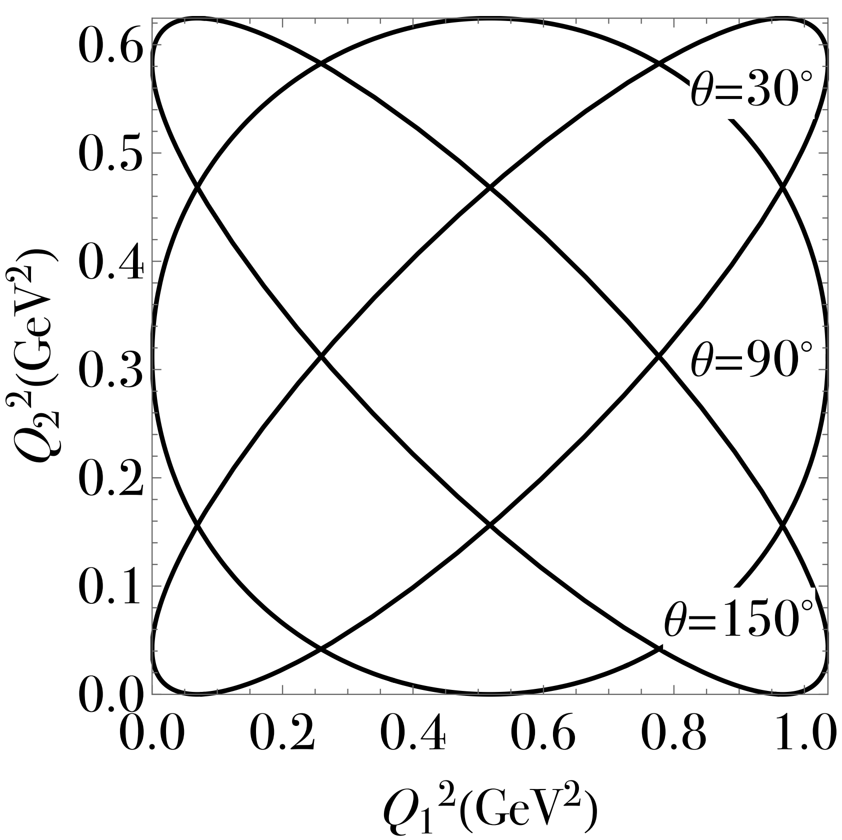


$Q^2_1 \simeq 0,\ Q^2_2 \neq 0$

$\downarrow$

$k \,//\, k_1$

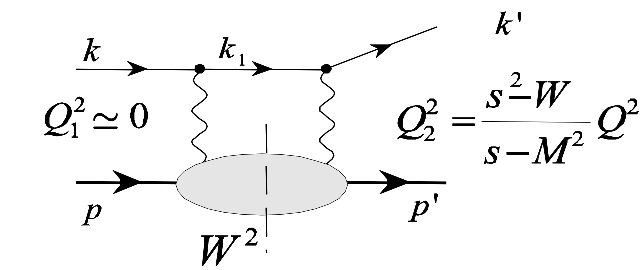


**Quasi - VCS**

$Q^2_1 \neq 0,\ Q^2_2 \simeq 0$

$\downarrow$

$k_1 \,//\, k'$

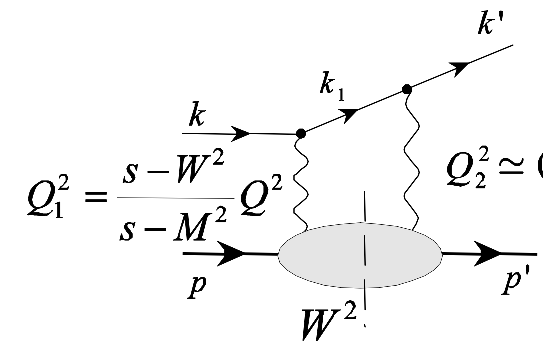


**Quasi - VCS**

$Q^2_1 \simeq 0,\ Q^2_2 \simeq 0$

$\downarrow$

$k_1 = 0,\ W = \sqrt{s} - m_e$

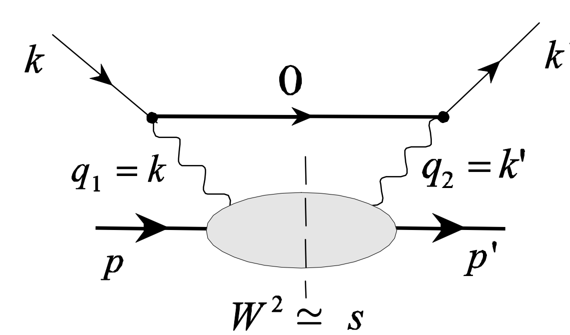


**Quasi - RCS**

## Kinematic enhancement for QRCS in $B_n$

- Pasquini & Vanderhaeghen (2004)
- Afanasev & Merenkov (2004)

# Quasi-Real Compton Scattering (QRCS)

$$\mathrm{SSA} = -\frac{\alpha\, Q^2}{\pi D(s,Q^2)} \int_{M^2}^{W^2_{\max}} dW^2\, \frac{|\vec{k}_1|}{4\sqrt{s}} \int_{-1}^{1} d\cos\theta_{k_1} \int_0^{2\pi} d\phi_{k_1}\, \frac{\mathrm{Im}\, L_{\rho\mu\nu} H^{\rho\mu\nu}}{Q_1^2\, Q_2^2}.$$

- Quasi-singular behaviour as $\mathrm{W} \to \mathrm{W}_{\max}$
- Two hard collinear photons
- Analogous to real Compton scattering

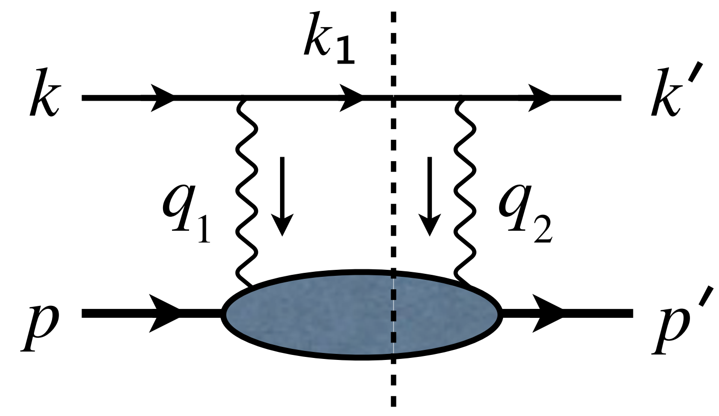


$$W_{\max} = \sqrt{s} - m_e, \quad E_{k_1} = m_e, \quad |\vec{k}_1| = 0$$

$$\text{At } W = W_{\max}: \qquad Q_1^2 = Q_2^2 = m_e \frac{W^2_{\max} - M^2}{\sqrt{s}}$$

- Slowly varying numerator and rapidly varying denominator for $\mathrm{W} \sim \mathrm{W}_{\max}$
- Strategy: numerator evaluated at $Q_1^2 = Q_2^2 = 0$ times

$$\frac{|\vec{k}_1|}{4\sqrt{s}} \int d\Omega_{k_1} \frac{1}{Q_1^2\, Q_2^2}$$

- This integral can be done analytically.
- Match to numerical solution for $\mathrm{W}$ below $\mathrm{W}_{\max}$

# Quasi-Real Compton Scattering (QRCS)

## Example above nominal threshold for N(1520)

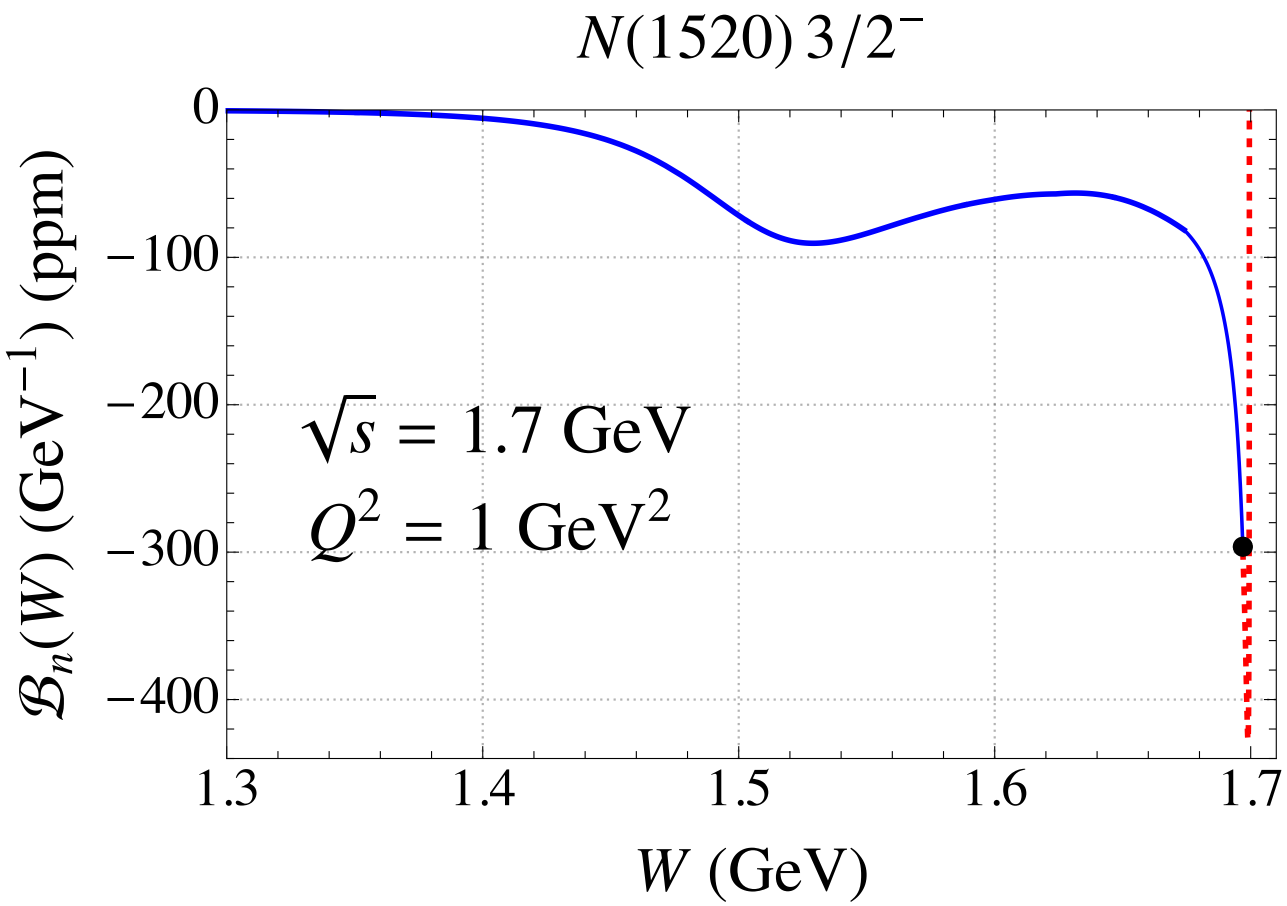


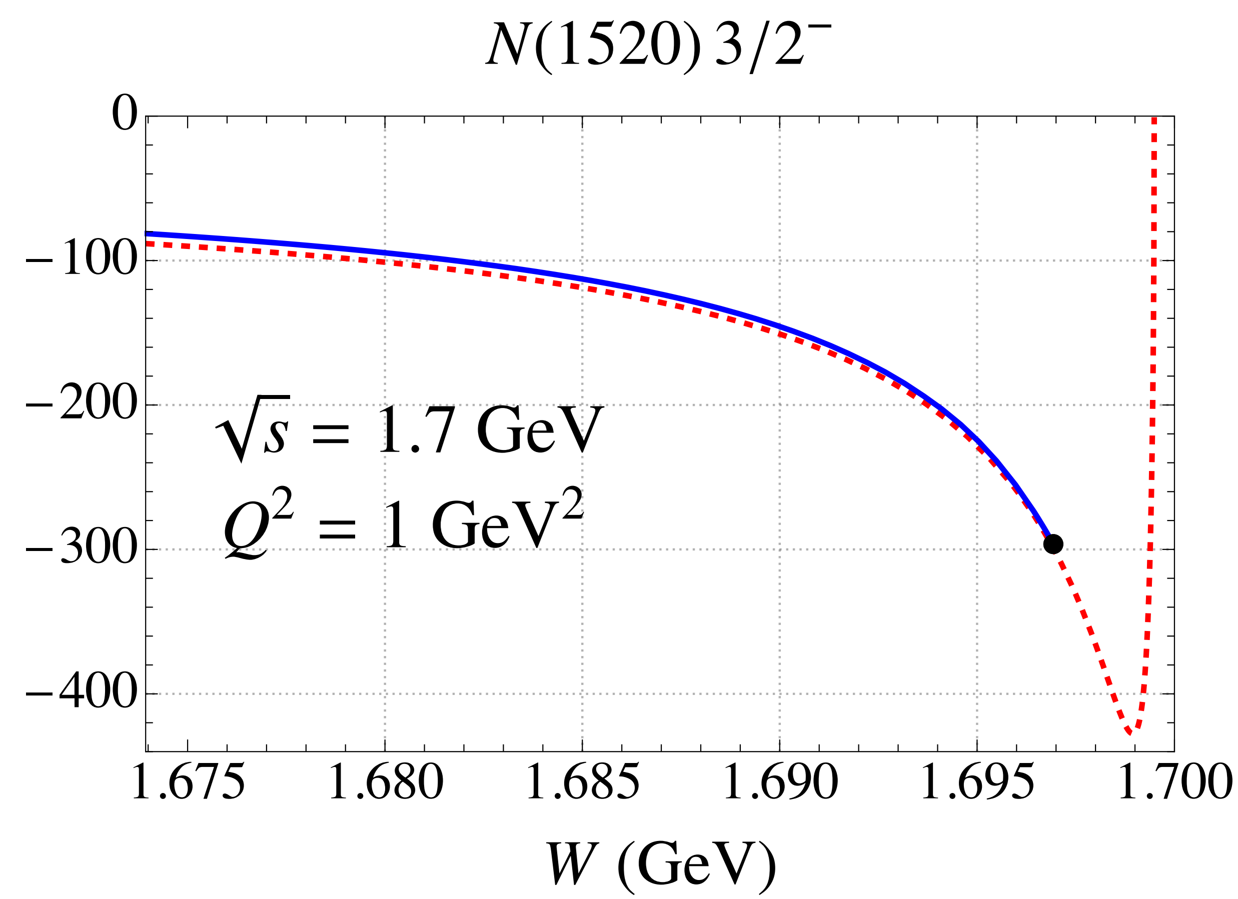


$$B_n = \int_{W_{\rm th}}^{W_{\rm max}} dW \ \mathcal{B}_n(W)$$

Match to numerical solution at $W^2 = \sqrt{s} - 5m_e$

# Beam normal SSA: fixed $E$ vs $\theta$

Ahmed, Blunden, Melnitchouk (arXiv:2306.02540)

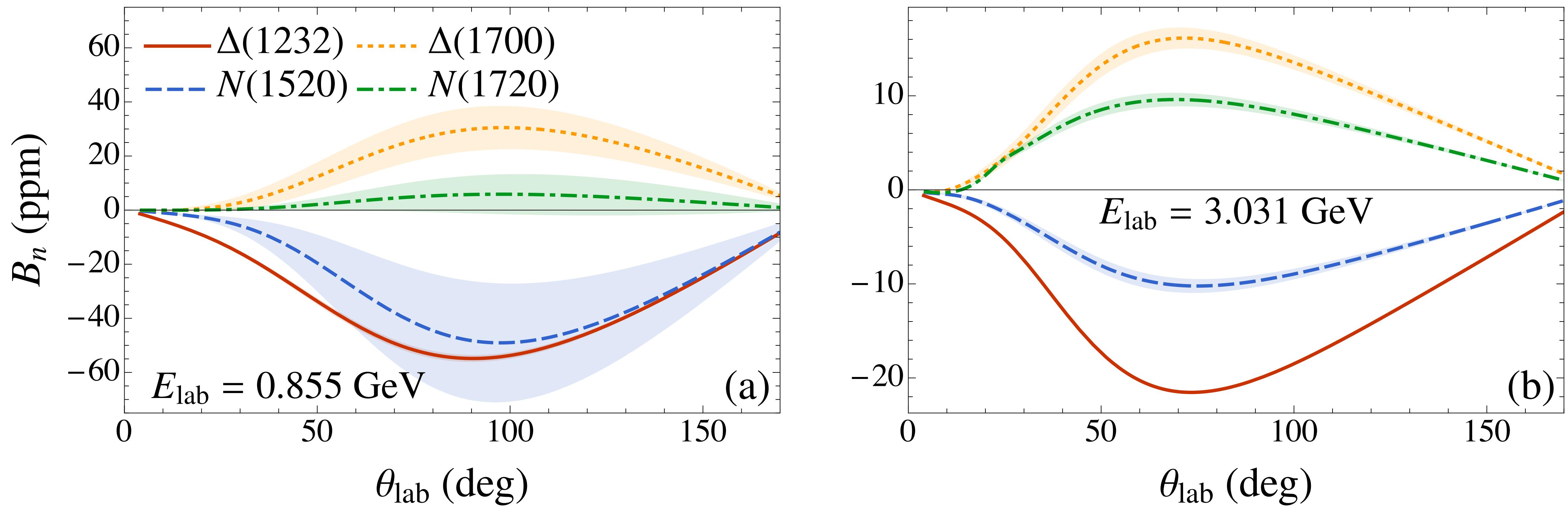


- Individual contributions from four largest spin $3/2$ resonances
- Decreases as $E$ increases
- Spin $1/2$ contributions suppressed by an order of magnitude
- Significant cancellation between positive parity ($\Delta(1232)$, $N(1520)$) and negative parity ($\Delta(1700)$, $N(1720)$) resonances

# Beam normal SSA: fixed $E$ vs $\theta$

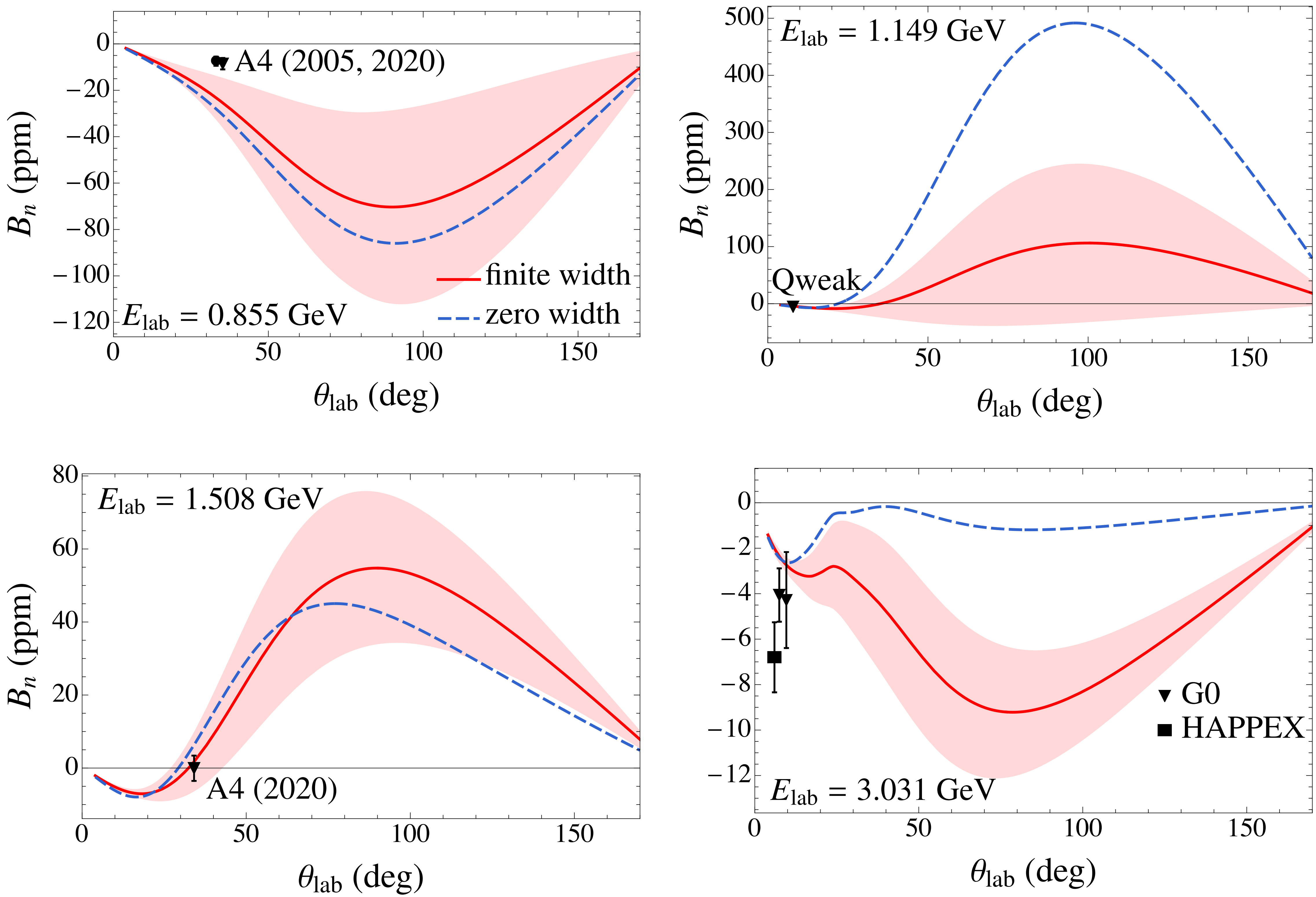


- Tends to overshoot data at low energies and forward angles
- Tends to undershoot data at high energies and forward angles

# Qweak data point magnified

- Afanasev & Merenkov (2004)
- Pasquini & Vanderhaeghen (2004)
- Gorchtein (2006)

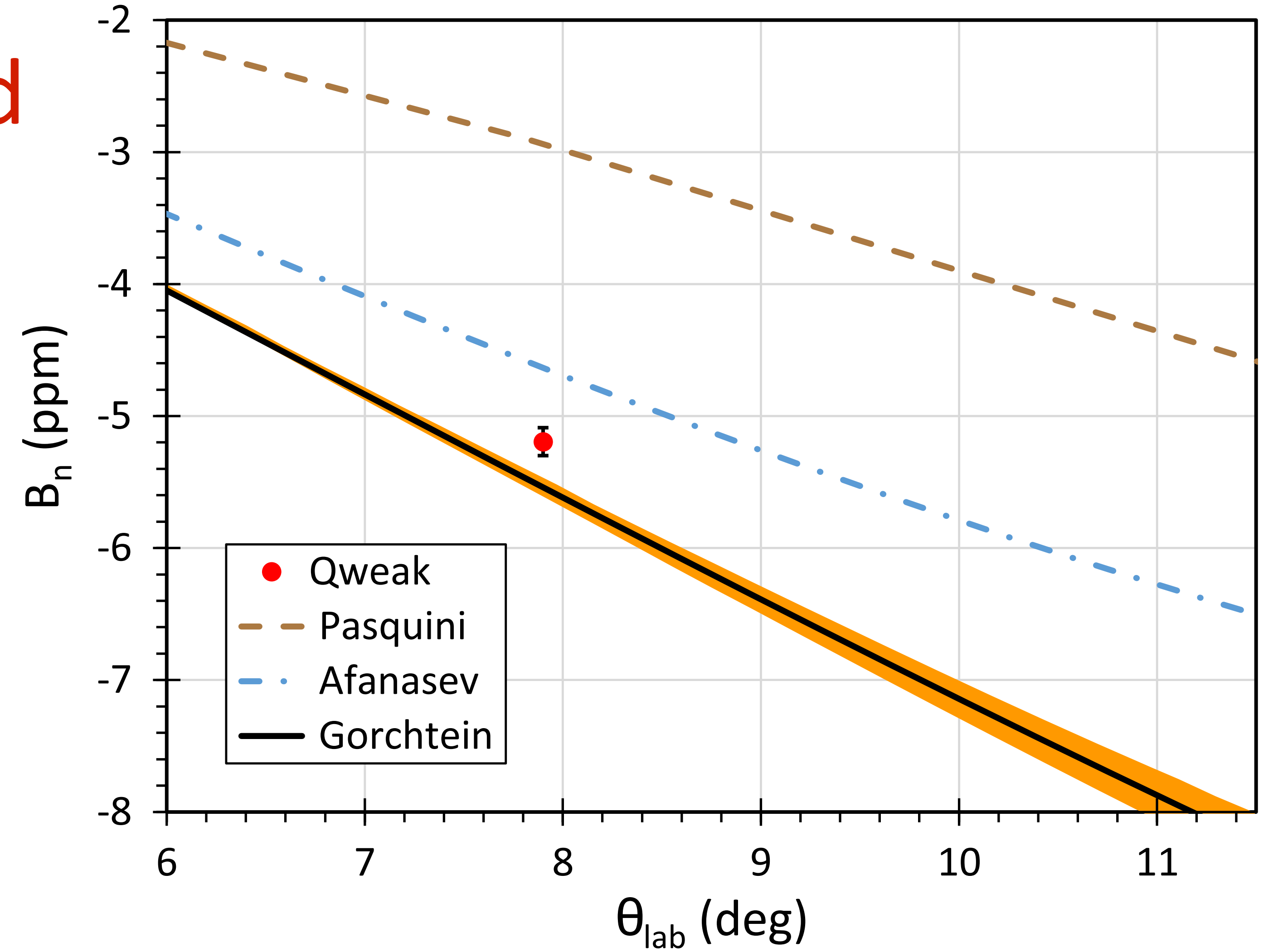


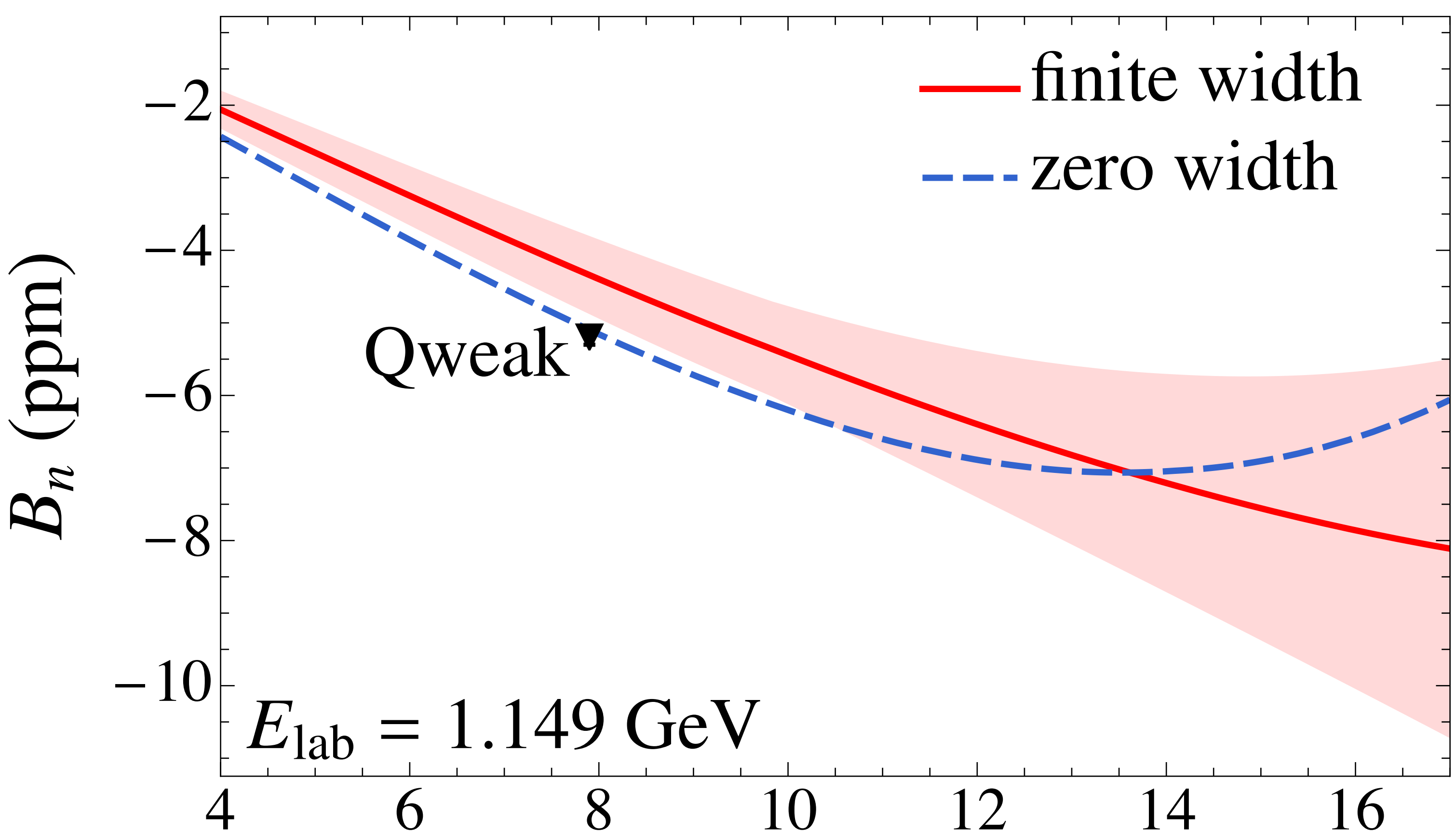


- Comparable with Afanasev and Gorchtein results
- Data point provides strong constraint on theory

# Beam normal SSA: fixed $\theta$ vs $E$

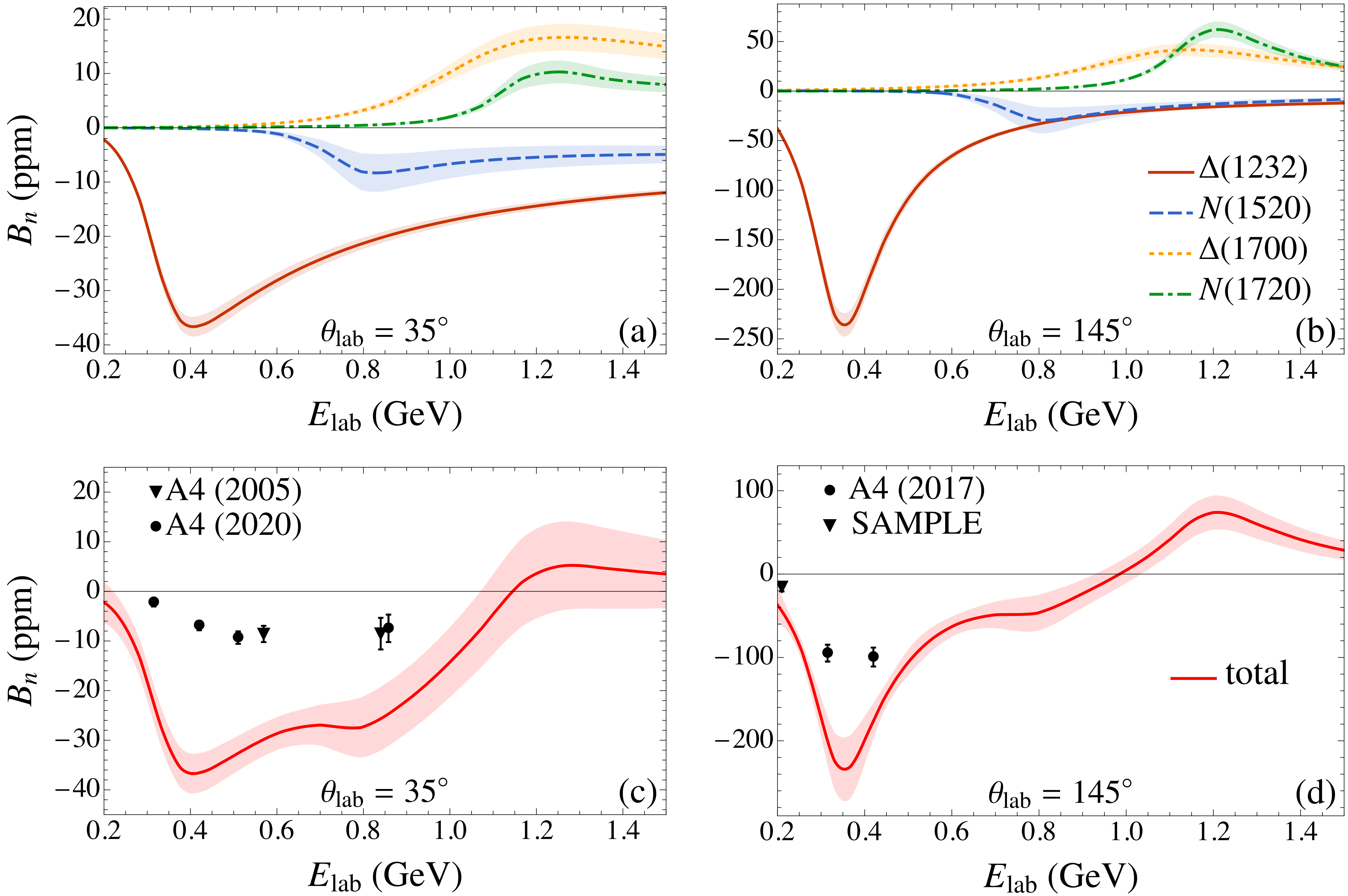


- Nominal threshold energy is at resonance peak in top row
- Tends to overshoot data in subthreshold region (low $E$)

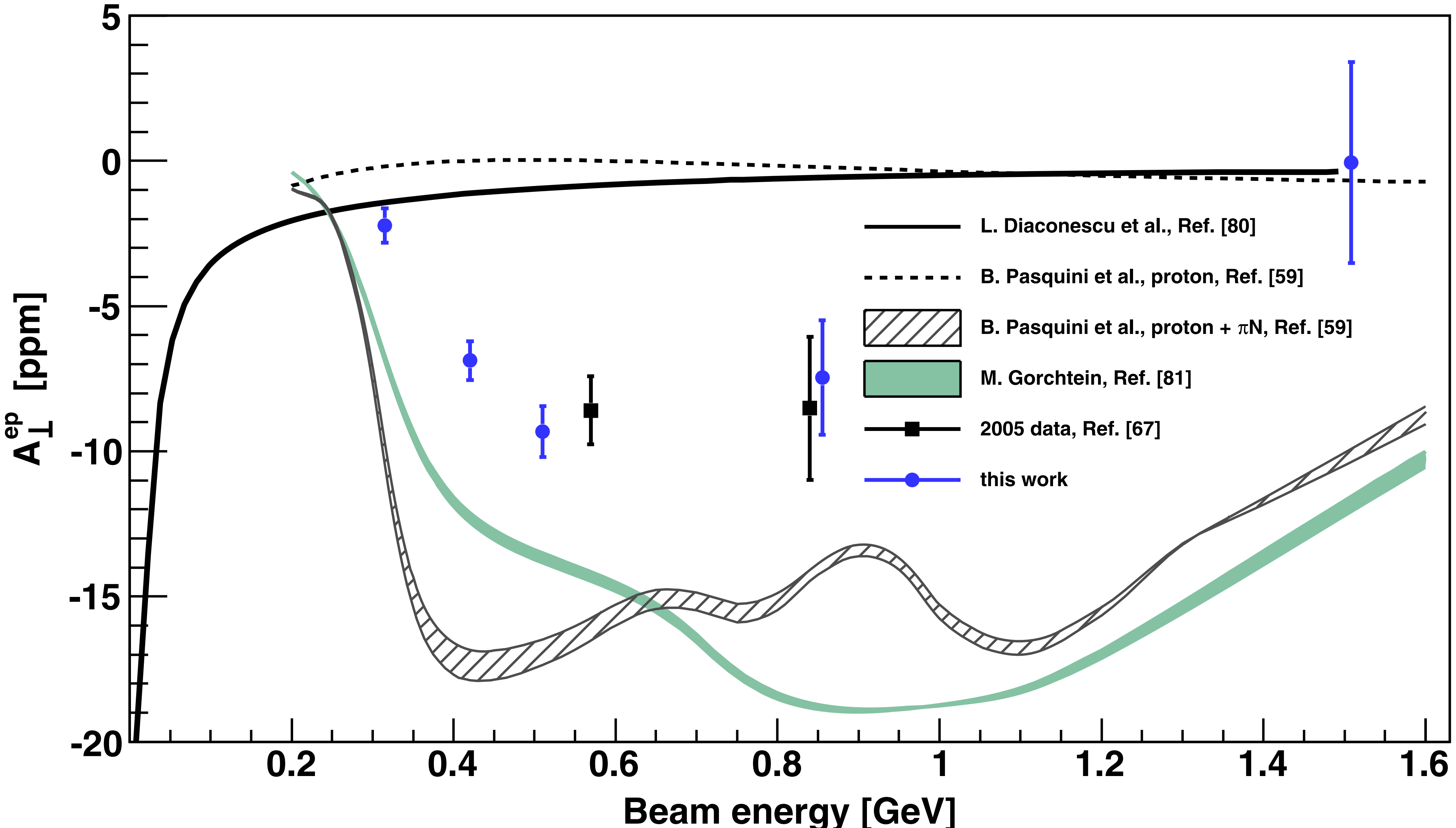


Guo *et al.*, PRL**124**, 122003 (2020)

Similar overshoot of data at low energy is seen in other work

# Target normal SSA

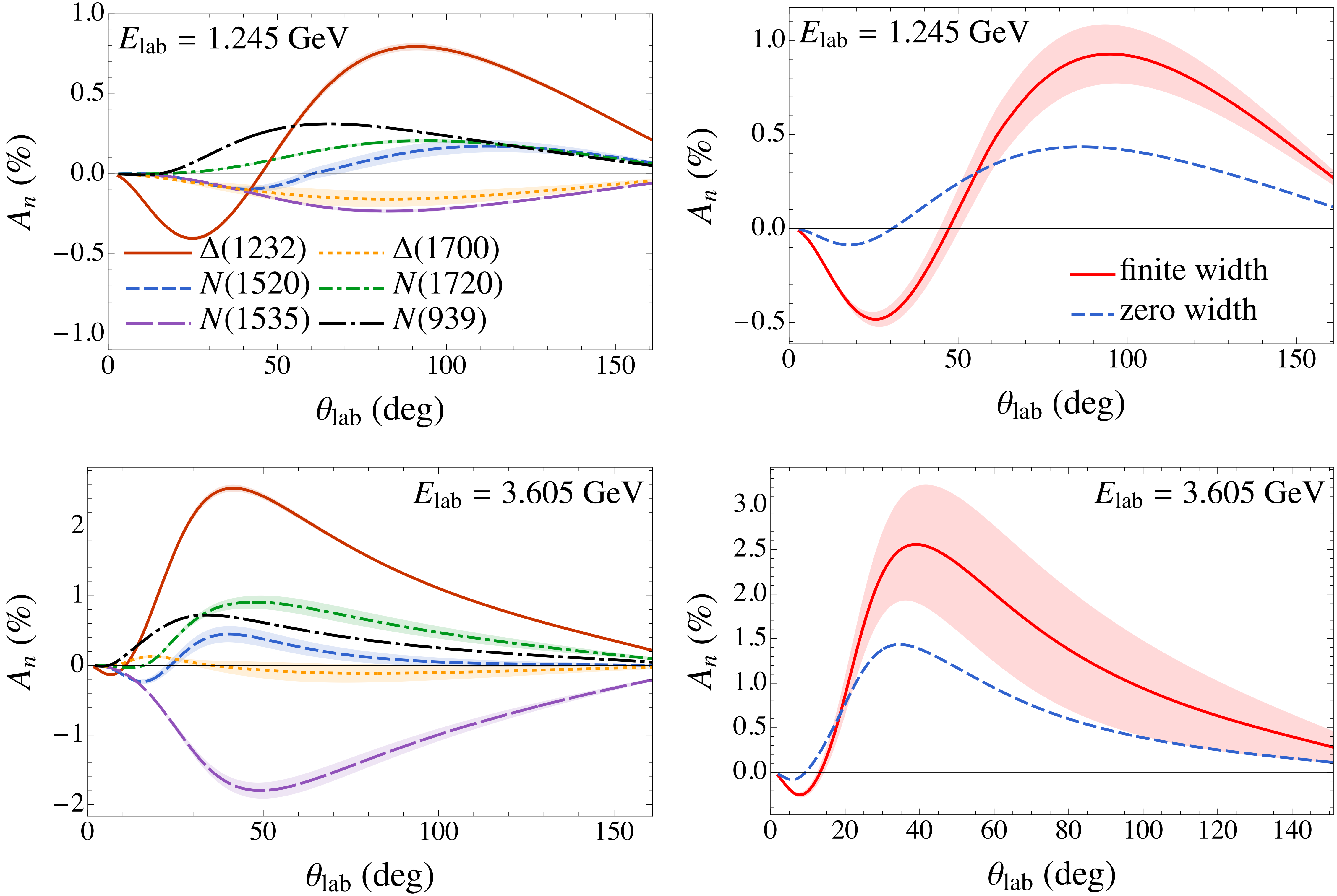


- Free of kinematics enhancements at thresholds (*i.e.* $W^2 \approx s$ )
- Moderate dependence on width
- Increases as $E$ increases (opposite of beam normal SSA)

# Form factors and the $G_E/G_M$ ratio

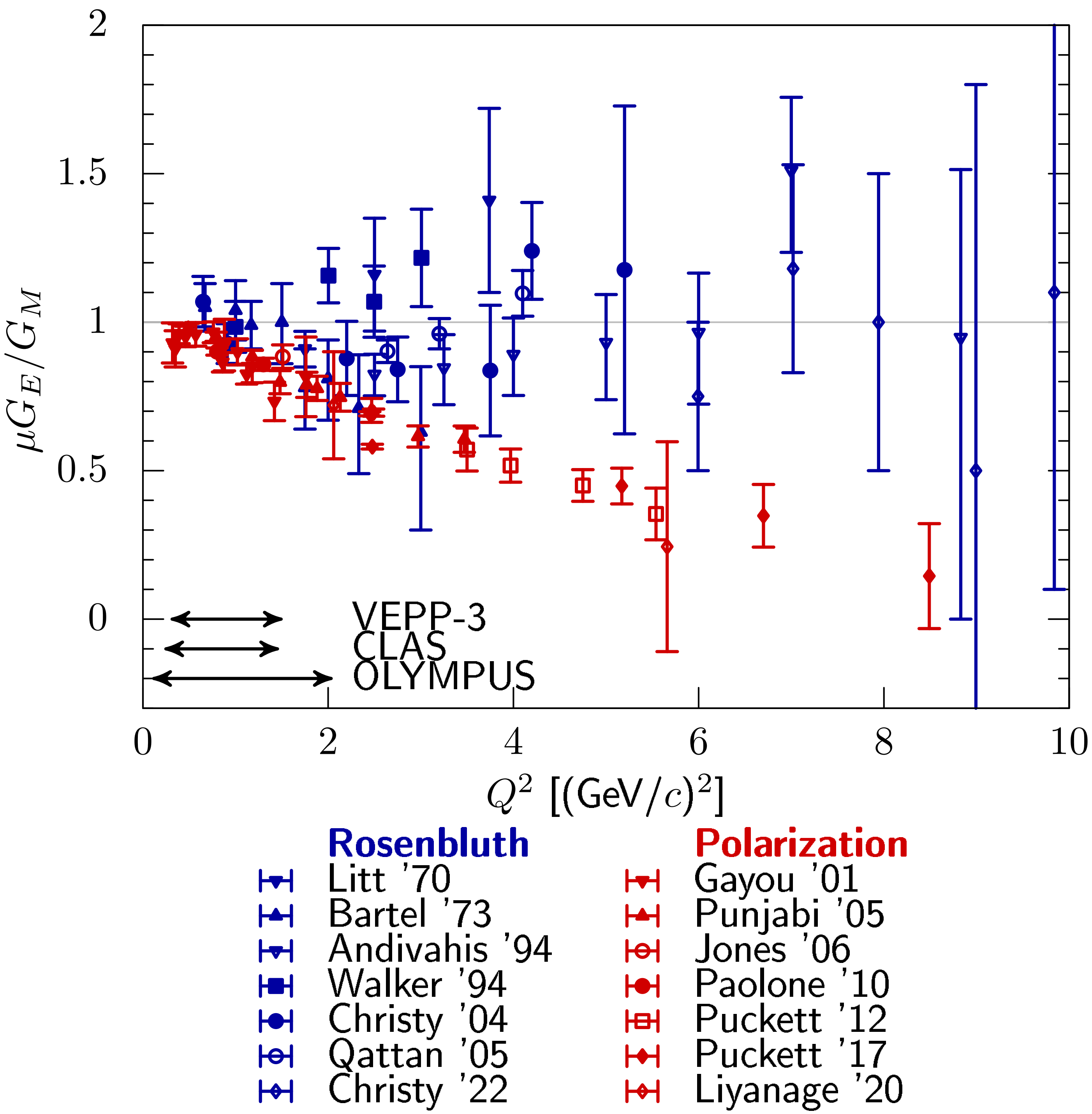


TPE leading candidate to explain discrepancy

# TPE corrections to cross section (CLAS resonances)

Ahmed, Blunden & Melnitchouk, PRC**102**, 045205 (2020)

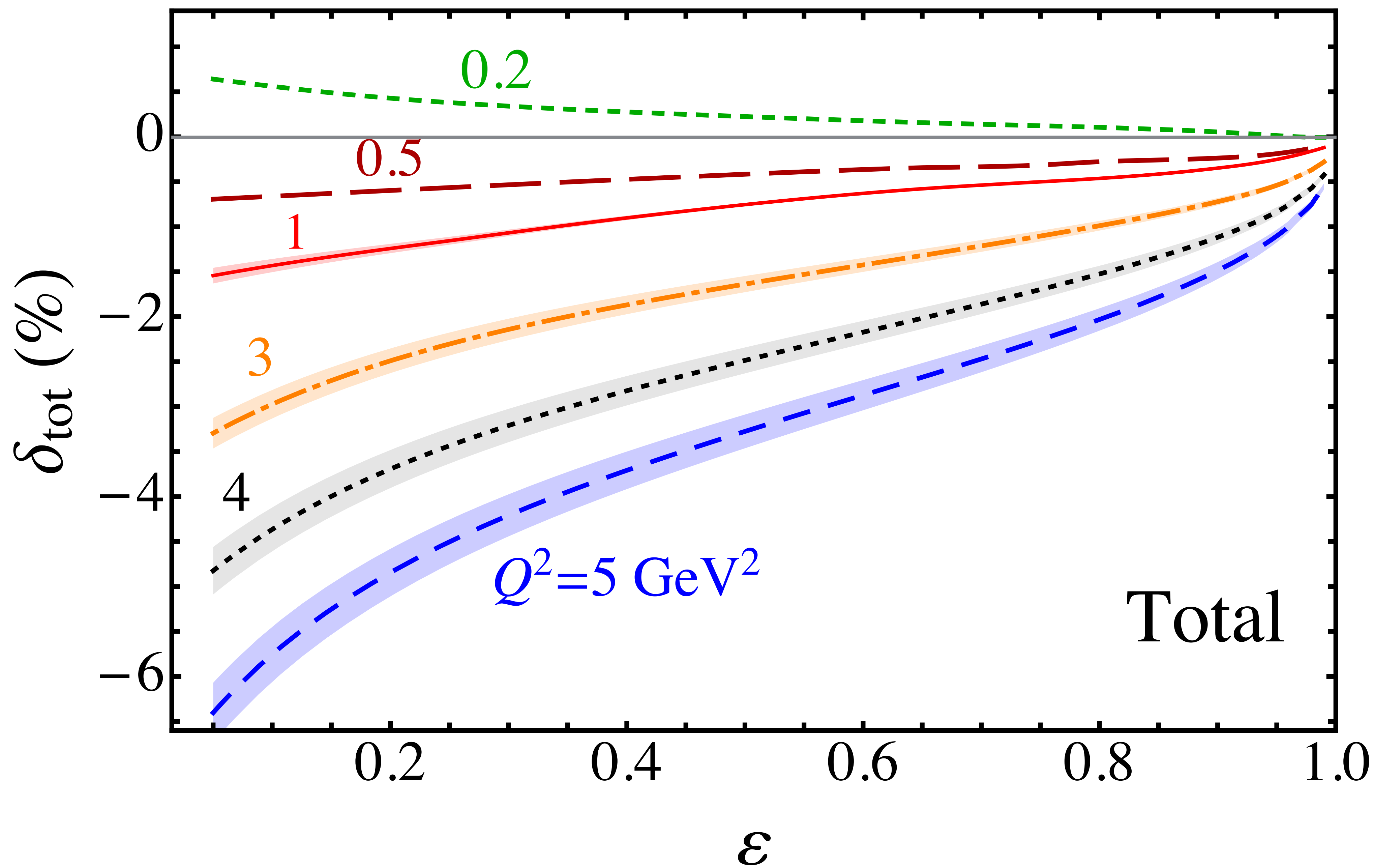


- Linear over mid-range of $\varepsilon$ values, but curves towards endpoints
- Presence of TPE allows for smaller contribution of $G_E^2$ to

$$\frac{1}{\tau}\sigma_{\rm red} = G_M^2 + \frac{\varepsilon}{\tau} G_E^2$$

$$\frac{1}{\tau}\sigma_{\text{red}} = G_M^2 + \frac{\varepsilon}{\tau}G_E^2$$

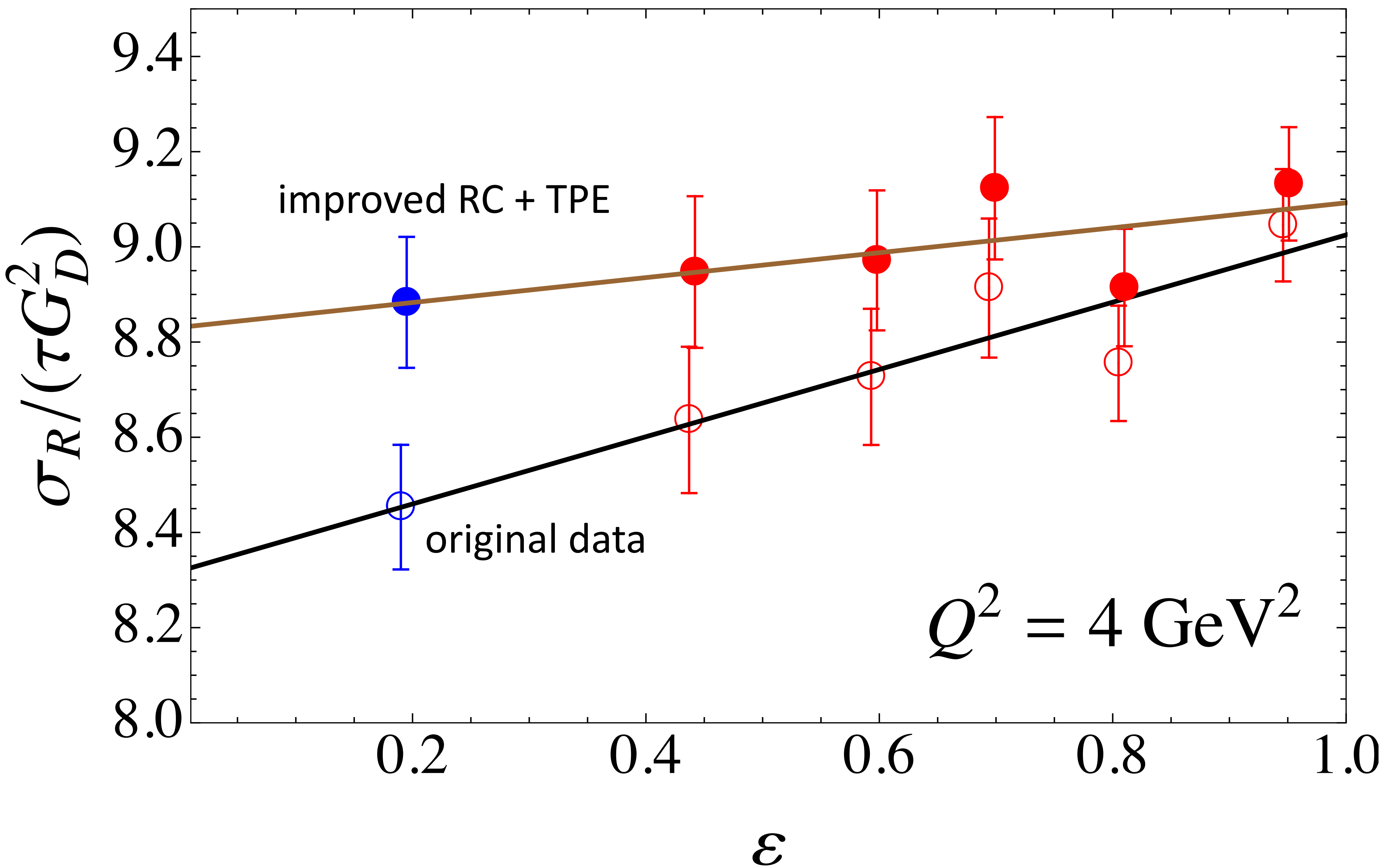


- Example from Andivahis data set at $Q^2 = 4\ \mathrm{GeV}^2$
- Uses improved RC + our TPE
- No evidence of non-linearity

# Summary

- Beam normal SSA interesting and challenging
  - Dominated by spin $3/2$
  - Mutual cancellation between opposite parities
  - Seems to overestimate data at low energies (where $\Delta(1232)$ dominates) and underestimate data at high energies
- Target normal SSA lack of data
- Efforts underway to incorporate electroproduction data throughout the resonance region, including non-resonant background, using CLAS data as input (Tomalak *et al.* have a similar approach using MAID analysis)